Horný L., Petřivý Z., Sobotka Z., Kohan M., Balint T., Chlup H., Kronek J., Mendová K., Hudák R., Schnitzer R., Danko M., Hlubeňová J. (2025) Notes on constitutive modeling of 3D-printed PLA materials. *Journal of the Mechanical Behavior of Biomedical Materials* Vol. 169, art. no. 107083. **Accepted manuscript** version distributed under CC BY-NC-ND 4.0. Link to the publisher version https://doi.org/10.1016/j.jmbbm.2025.107083.

Notes on constitutive modeling of 3D-printed PLA materials

Lukáš Horný[1*], Zdeněk Petřivý[1], Zbyněk Sobotka[1], Miroslav Kohan[2], Tomáš Balint[2], Hynek Chlup[1], Jakub Kronek[1], Katarína Mendová[1], Radovan Hudák[2], Marek Schnitzer[2], Mária Danko[2], Jana Hlubeňová[2]

[1]Czech Technical University in Prague, Faculty of Mechanical Engineering, Technická 4, Prague 160 00, Czech Republic

[2]Technical University of Košice, Faculty of Mechanical Engineering, Letná 9/B, 042 00 Košice, Slovakia

*Corresponding author: Lukáš Horný, lukas.horny@fs.cvut.cz

Abstract: Materials based on polylactic acid (PLA) are now extensively utilized across various fields, including biomedical engineering, where they are increasingly favored for the development of implantable devices and tissue replacements. Due to its ease of melting, PLA is also among the most commonly used materials in 3D printing. This makes PLA-based materials highly attractive for the production of customized implants and personalized medical devices. To support the design of such components, the computer simulations involved must rely on reliable constitutive models. The current approaches for PLA-based 3D printed material models include linear elasticity, linear viscoelasticity or elastoplasticity, hyperelasticity, and advanced nonlinear theories dealing with irreversible processes. While linear theories are undoubtedly simplistic, nonlinear models frequently result in complex descriptions which are dependent on too many material parameters. In this context, our study aims to show the ability of the Quasi-Linear Theory of Viscoelasticity to accurately reproduce the tensile test results for PLA-based materials produced using Fused Deposition Modeling. We will demonstrate this with tensile test results performed on PLA-PHB strips with TAC added as a plasticizer. The nonlinear stress-strain curves obtained from the experiments were successfully fitted by using a model compatible with finite strain theory, comprising only three material parameters. One of these parameters relates to equilibrium elasticity, while the other two correspond to the Maxwell element, which describes dissipative behavior. These results highlight the potential of this modeling approach to capture the essential aspects of the mechanical response using a minimal parameter set, which offers a promising balance between simplicity and predictive power for applications in simulation-based design.

Keywords: Additive manufacturing, Constitutive model, Polyhydroxybutyrate, Polylactic acid, Tensile test, QLV.

1. Introduction

Materials based on polylactic acid (PLA) are now widely used in various fields, including biomedical engineering, where they are increasingly popular in the development of implantable devices and tissue replacements (Lasprilla et al., 2012; Saini et al., 2016; Grémare et al., 2018; Siyajeu et al., 2023; Gao and Drozdov, 2024). Notably, PLA's relatively good biocompatibility makes it advantageous for medical applications (Onuki et al., 2008; Ramot et al., 2016; Saini et al., 2016; Shilov et al., 2022; Trebuňová et al., 2023). Another appealing property of PLA is its degradability, which can be beneficial in designing implants intended to serve as temporary supports until the body replaces them with newly formed tissue (Weir et al., 2004; Madhavan Nampoothiri et al., 2010; Pelegrini et al., 2016; Findrik Balogová et al., 2021; Horný et al., 2025).

The physical and chemical properties of PLA materials, along with the aforementioned degradability, significantly depend on the production method employed (Farah et al., 2016). For instance, macroscopic mechanical properties such as strength and elasticity can vary dramatically depending on whether we are working with membranes, bands, or tubes prepared by electrospinning which are designed for interaction with soft tissues, or with parts created through 3D printing - typically using Fused Deposition Modeling (FDM) technology - intended for orthopedic or dental applications (Sankaran et al., 2014a; Lopresti et al., 2020; Grémare et al., 2018; Vukasovis et al., 2019; Kechagias and Zaoutsos, 2023; Kohan et al. 2022; Dukle and Sankar, 2024a; Horný et al., 2025). To illustrate, Lopresti et al. (2020) reported that the Young's modulus for spatially omnidirectional PLA electrospun material ranges from 5 to 20 MPa, while FDM-printed strips achieve a Young's modulus of approximately 3000 MPa (Vukasovic et al., 2019). In terms of strength Sankaran et al. (2014b), for example, reported an average strength of 11.19 MPa for PLA scaffolds used in cardiovascular engineering, Vukasovic et al. (2019) recorded an ultimate tensile strength ranging from 50 to 70 MPa in 3D-printed materials.

When focusing specifically on 3D-printed products, substantial differences in mechanical properties can still be observed depending on the particular 3D-printing technology employed. The FDM technique used in our study to produce specimens for mechanical testing is widely favored due to its low cost, ease of use, and ability to rapidly fabricate customized geometries from biocompatible and biodegradable materials such as PLA. These features make FDM particularly attractive for applications in biomedical engineering and the development of personalized implants. However, FDM also presents certain limitations. Surface finish and dimensional accuracy may pose a challenge (Fountas et al., 2022) and can fall short compared to photopolymerization-based methods such as PolyJet or stereolithography (Abdulhameed et al., 2009). Regarding the mechanical properties examined in this work, namely elasticity and strength, they are highly sensitive, besides infill rate, to process parameters such as printing temperature, layer thickness, and interlayer bonding quality and porosity (Fountas et al., 2023; Seyedsalehi et al., 2021).

Moreover, the dispersion of these properties is also due to the fact that PLA is mostly used in combination with other molecules and materials. These combinations can take place at various length scales, such as the nano-scale, where copolymers are formed, the micro-scale, where composites are formed, or the macro-scale, where materials are combined as a sandwich construction. At the nano-scale, for example, lactic acid is successfully combined with ε-caprolactone, which typically reduces the stiffness of the resulting material, as PLA itself is relatively stiff compared to polycaprolactone (PCL) (Mikes et al., 2021). Their copolymer, poly(L-lactide-co-ε-caprolactone), frequently referred to as PLCL, has been reported as a promising material for the development of vascular replacements (Sankaran et al., 2014a; Horakova et al., 2018; Ozdemir et al., 2024; Horný et al., 2025). At the macroscopic level, which corresponds to the use of 3D printing or extrusion technology, the stiffness of PLA can be mitigated by incorporating polyhydroxybutyrate (PHB), which, like PLA, is an aliphatic polyester but demonstrates an even better degradation profile than PLA (Findrik Balogová et al., 2021; Kohan et al., 2022; Čajková et al., 2024).

As mentioned earlier, 3D-printed PLA materials are typically relatively stiff from a biomechanical perspective (Farah et al., 2016). Their tensile curves exhibit a nonlinear stress-strain relationship (Vukasovic et al., 2019; Custodio et al., 2021; Volgin and Shishkovsky, 2021; Luo et al., 2022; Afshar et al., 2023; Mrozik and Pejkowski, 2023; Fountas et al., 2023; Zaoutsos and Kechagias, 2025), which is a characteristic they share with PLA materials obtained through electrospinning (Dai et al., 2018; Lopresti et al., 2022; Viera et al., 2024) although the magnitude may differ due to disparate stiffnesses. A concave stress-strain curve, typical of FDM-processed PLA material, resembles the mechanical behavior observed in industrial thermoplastics (Rösler et al., 2007; Brinson and Brinson, 2008; Bergström, 2015). In contrast to linear elasticity, where the data allow for a unique interpretation leading to the Young's modulus or, more generally, to the tensor of elastic constants, the nonlinear case is complicated by the fact that the components of the elasticity tensor are no longer constants.

When the material response is considered elastic, the hyperelasticity theory is often utilized (Holzapfel, 2000), particularly for finite deformations. Hyperelastic materials are described by the elastic potential W, which represents the strain energy density, and the stress tensor components are obtained as

Horný L., Petřivý Z., Sobotka Z., Kohan M., Balint T., Chlup H., Kronek J., Mendová K., Hudák R., Schnitzer R., Danko M., Hlubeňová J. (2025) Notes on constitutive modeling of 3D-printed PLA materials. *Journal of the Mechanical Behavior of Biomedical Materials* Vol. 169, art. no. 107083. **Accepted manuscript** version distributed under CC BY-NC-ND 4.0. Link to the publisher version https://doi.org/10.1016/j.jmbbm.2025.107083.
derivatives of W with respect to the strain tensor components (Holzapfel, 2000; Bergström, 2015). An even more complex description of the behavior is required if we want to consider the dissipative processes that manifest as viscoelasticity, elastoplasticity or viscoelastoplasticity (Bergström 2015). Each of these scenarios can arise in the mechanical behavior of PLA-based 3D printing materials, and the choice of theory depends on the specific objectives of the study.

The linear elasticity theory is most frequently employed by authors focusing on materials science rather than mechanics per se. In these cases, articles often report elastic constants determined at the origin of the tensile curve (Vukasovic et al., 2019; Gonabadi et al., 2020; Rajpurohit et al., 2022). Small-strain theory is also occasionally applied in papers utilizing elastoplastic models (Monaldo et al., 2023; Zarna et al., 2023), linear viscoelastic models (Issabayeva and Shishkovsky, 2023), and within nonlinear contexts (Luo et al., 2022; Adibeig et al., 2023; Foroughi et al., 2023; Mrozik and Pejkowski, 2023; Ji et al., 2024). However, models based on infinitesimal strains cannot be reliably used at finite strains, as they do not satisfy objectivity requirements (Holzapfel, 2000). The hyperelastic theory, sometimes used to express the material nonlinearity of PLA-based 3D printed materials (Asfahr et al., 2023; Issabayeva and Shishkovsky, 2023; Zarna et al., 2023), is compatible with objectivity requirements. However, it does not account for irreversible phenomena such as creep or stress relaxation (Holzapfel, 2000; Bergström, 2015). A fully nonlinear viscoelastoplastic description, like the Three Network Model (Bergström, 2015; Volgin and Shishkovsky, 2021), is rare, perhaps due to its complexity.

While PLA-based materials are known for their nonlinear behavior, especially under large deformations, there is a lack of comprehensive viscoelastic models that can capture both the material's time-dependent and nonlinear mechanical responses. Therefore, the primary motivation of this paper is to demonstrate, through the most elementary possible example, how a relatively simple constitutive model that is compatible with finite strain theory and allows for viscoelastic phenomena will describe the nonlinear tensile curves obtained for a 3D-printed PLA material. In the following sections, Fung's theory of Quasi-Linear Viscoelasticity (QLV), which is based on the multiplicative decomposition of relaxation effects and material nonlinearity, will be applied. FDM printed PLA-PHB strips, prepared in our laboratory, will be used to demonstrate the capability of QLV. Incorporating such a viscoelastic model enables more accurate predictions of PLA's performance in real-world applications, including biomedical implants, where both elastic and viscoelastic properties influence the material's functionality.

2. Materials and Methods

2.1 PLA-PHB specimens

Samples for mechanical testing were prepared using FDM (also known as Fused Filament Fabrication, FFF) 3D printing technology at the Department of Biomedical Engineering and Measurement of the Faculty of Mechanical Engineering of the Technical University of Košice, Slovakia. The filament, with a diameter of 1.75 mm, was developed in house from pellets using the Filament Maker Composer series 450 (3devo, The Netherlands). It was composed of a blend containing PLA (85 wt%, Purasorb®, Corbion, Netherlands) and PHB (15 wt%, Biomer® P300, Biomer, Germany), to which Tricytyl-2-Acetyl Citrate (TAC, 25-30 wt%) was added as a plasticizer (TAC used in this blend was purchased from two suppliers: Foconsci Chemical Industry, China, and CD Formulation, USA). The filament production process is illustrated in Figure 1.

Horný L., Petřivý Z., Sobotka Z., Kohan M., Balint T., Chlup H., Kronek J., Mendová K., Hudák R., Schnitzer R., Danko M., Hlubeňová J. (2025) Notes on constitutive modeling of 3D-printed PLA materials. *Journal of the Mechanical Behavior of Biomedical Materials* Vol. 169, art. no. 107083. **Accepted manuscript** version distributed under CC BY-NC-ND 4.0. Link to the publisher version https://doi.org/10.1016/j.jmbbm.2025.107083.

Samples were printed as rectangular strips measuring 5 mm x 1 mm x 120 mm (width x thickness x length) from the PLA-PHB filaments using a DeltiQ2 printer (Trilab, Czech Republic). Fig. 1A documents the printing process. The PLA-PHB samples for the mechanical experiments were prepared in four distinct batches, labeled A to D. These batches varied in terms of plasticizer proportion (A vs. B), plasticizer manufacturer (B vs. C), and the printing infill density (A vs. D). Detailed differences between the groups are provided in Table 1. For all samples, the extruder temperature was set to 175 °C, and the printing speed was maintained at 30 mms^{-1}. A rectilinear structure was chosen for the infill.

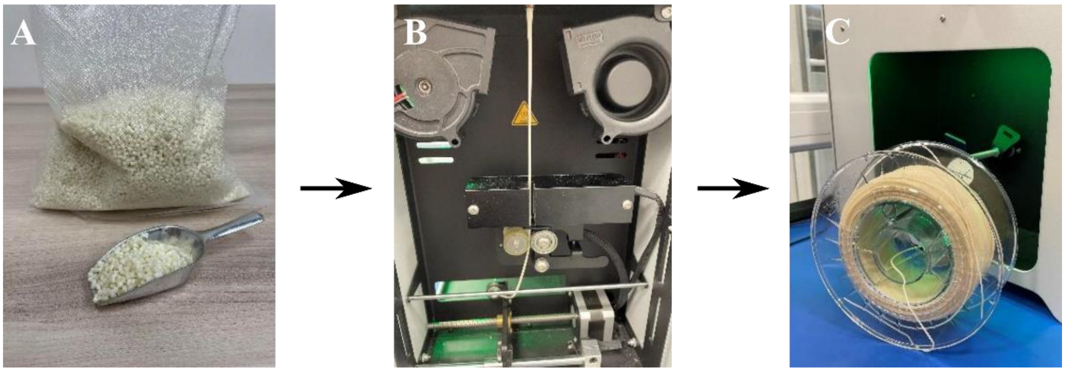

Fig. 1 Preparation of material for 3D printing from polymer granules (A) by mixing, melting, and extrusion (B) into the resulting filament (C).

Table 1. Summary of the experimental specimens.

Group	Samples	Infill [%]	PLA [wt%]	PHB [wt%]	TAC [wt%]	Suppliers
A	6	100	85	15	25	Purasorb-Biomer-FCI
B	6	100	85	15	30	Purasorb-Biomer-FCI
C	6	100	85	15	30	Purasorb-Biomer-CDF
D	5	50	85	15	25	Purasorb-Biomer-FCI

FCI = Foconsci Chemical Indrustry, CDF = CD Formulation

2.2 Uniaxial tensile tests

A monotonous uniaxial tensile test was conducted in order to characterize the mechanical response of the PLA-PHB samples. The experiments were performed using a Zwick/Roell multipurpose tensile testing machine (Zwick/Roell, Germany), specifically designed for the testing of soft tissues and polymeric materials. The applied force was measured by HBK U9C +/- 25N (accuracy class 0.2; Hottinger Brüel & Kjær, Germany) force transducers, and the deformation of the samples during testing was recorded by a built-in video-extensometer (5MPx camera IDS uEye 3.0; IDS, Germany) at a 20 Hz sampling rate. The printed samples were cut in half to create two testing specimens, each measuring 60 mm in length. The experiments were conducted at a loading rate of 0.2 mms^{-1}, resulting in a deformation rate of approximately 0.004 s^{-1}, until specimen failure occurred. The ultimate tensile strength (P_{max}) was determined as the maximum force divided by the reference cross-sectional area. A specimen mounted in the machine is depicted in Fig. 2B.

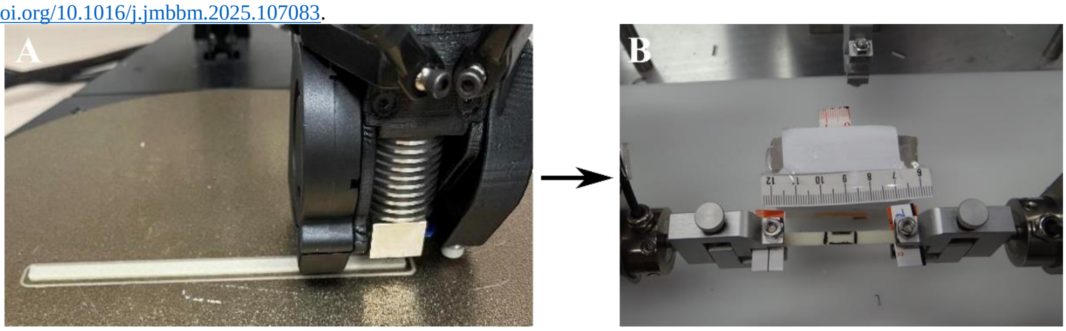

Fig. 2 – Printing of the PLA-PHB specimen (A), the specimen in the testing machine (B).

2.3 Constitutive model

The primary objective of our paper is to demonstrate that Quasi-Linear Viscoelasticity (QLV) theory can accurately reproduce the nonlinear strain curves observed during the mechanical testing of FDM-fabricated PLA-based materials. QLV was introduced by Y. C. Fung in the 1970s, and a detailed explanation can be found in Fung's original works (Fung, 1972, 1993, 1994) as well as in standard monographs on viscoelasticity and constitutive modeling (Drapaca et al., 2007; Wineman, 2009; Merodio and Ogden, 2020). Recent applications of QLV in tissue biomechanics are documented in studies by De Pascalis et al. (2014, 2018) and Petřivý and Horný (2022).

QLV employs the standard Boltzmann integral, which is formulated within the framework of finite strain theory. The fundamental idea is that viscous effects and material nonlinearity can be separated and are assumed to be mutually independent. The general QLV constitutive equation in symbolic notation is expressed in (1). Here, **S** denotes the second Piola-Kirchhoff stress tensor, t represents the time at which the mechanical response is evaluated, whereas τ is the time associated with the deformation history. $\mathbf{S}^e$ denotes the second Piola-Kirchhoff stress corresponding to the elastic response of the material which is determined from the elastic potential W. Tensor **G** represents the reduced relaxation function and, in its most general form, is a fourth-order tensor that characterizes the viscous part of the material response.

$$\mathbf{S}(t)=\int_{-\infty}^{t}\mathbf{G}(t-\tau)\frac{\partial\mathbf{S}^e(\tau)}{\partial\tau}d\tau \tag{1}$$

Formulating the constitutive equation (1) using the second Piola-Kirchhoff stress is advantageous because the objectivity of the time derivative of the stress is immediately ensured since **S** is expressed in the material description (Holzapfel 2000). By using additive decomposition of the stress into the isochoric and deviatoric part, and applying the per partes integration rule, and incompressible behavior, (1) can be converted to the form of (2), which is expressed using the Cauchy stress $\boldsymbol{\sigma}$. In (2), **F** is the deformation gradient tensor, **I** is the second order identity tensor, p is hydrostatic stress component that must be determined from the boundary conditions, and G_D and $\mathbf{S}^e{}_D$ are the deviatoric part of the relaxation function G and the deviatoric part of the elastic stress $\mathbf{S}^e$. The algebraic manipulations involved in deriving equation (2) are somewhat lengthy and are detailed in Petřivý and Horný (2022) or De Pascalis et al. (2014).

$$\boldsymbol{\sigma}(t)=\mathbf{F}(t)\left(\mathbf{S}_D^e(t)+\int_0^t\frac{\partial G_D(t-\tau)}{\partial\tau}\mathbf{S}_D^e(\tau)d\tau\right)\mathbf{F}^T(t)-p(t)\mathbf{I} \tag{2}$$

To make the elastic part of the mechanical response compatible with finite strain theory, a hyperelastic description is employed. In such a case, equation (3) can be used to express $\mathbf{S}^e{}_D$ (De Pascalis et al., 2014).

$$\mathbf{S}_D^e = 2\left[W_1\mathbf{I} + \frac{1}{3}\left(I_2 W_2 - I_1 W_1\right)\mathbf{C}^{-1} - W_2\mathbf{C}^{-2}\right] \tag{3}$$

C is the right Cauchy-Green deformation tensor, $\mathbf{C} = \mathbf{F}^T\mathbf{F}$, I_1 and I_2 are the first and second principal invariants of **C**, and W_1 and W_2 are abbreviations for $\partial W/\partial I_1$ and $\partial W/\partial I_2$, respectively.

To keep the model as simple as possible, it was decided to employ very elementary form of functions expressing the mechanical response of the material. Thus, the elastic part of the mechanical response is described by neo-Hooke strain energy density function (4), and the relaxation behavior is represented by a single normalized exponential function (5). In (4), μ is the stress-like material parameter that, at infinitesimal strains, corresponds to the shear modulus. Similarly, in (5), g and τ_R are material parameters that, within the context of the linear viscoelasticity theory, can be associated with the Maxwell element.

$$W = \frac{\mu}{2}\left(I_1 - 3\right) \tag{4}$$

$$G_D\left(t\right) = 1 - g\left(1 - e^{-\frac{t}{\tau_R}}\right) \tag{5}$$

2.4 Identification of material parameters

The material parameters were estimated using the NLPSolve optimization procedure implemented in Maple 2022 (MapleSoft, Canada). The objective function was defined as the sum of the squared errors between the stress predicted by the model, σ_{MOD}, and the experimental stress, σ_{EXP}, obtained as the measured force per deformed cross-section area. To document the success of the resulting estimates of the constitutive parameters, the coefficient of determination, R^2, was used, which represents a normalized measure of agreement between the model and the observations and is based on the objective function used. Based on the incompressibility assumption, the Cauchy stress under uniaxial tension is given by $\sigma_{EXP} = F\lambda/S_0$, where F is the measured force, S_0 is the reference cross-sectional area, and λ is the stretch obtained as the ratio of the deformed to the initial distance between marks on the specimen. σ_{MOD} is obtained by substituting (4) and (5) into (2) with the simultaneous application of (3), resulting in the final expression given in (6).

$$\sigma\left(t\right) = \frac{2}{3}\mu\lambda^2\left(t\right)\left(1 - \frac{1}{\lambda^3\left(t\right)} - \frac{g}{\tau_R}\int_0^t\left(1 - \frac{1}{\lambda^3\left(\tau\right)}\right)e^{-\frac{t-\tau}{\tau_R}}d\tau\right) - \frac{\mu}{3\lambda\left(t\right)}\left(1 - \lambda^3\left(t\right) - \frac{g}{\tau_R}\int_0^t\left(1 - \lambda^3\left(\tau\right)\right)e^{-\frac{t-\tau}{\tau_R}}d\tau\right) \tag{6}$$

The NLPSolve (Non-Linear Program Solve) procedure in Maple 2022 used for parameter identification was relatively fast and delivered stable convergence within several minutes per task on a workstation with 32 GB DDR5 RAM, 1 TB SSD, and 16-core 4.1 GHz CPU (Windows 11).

2.5 Statistical analysis

In order to verify the existence of differences between the results of tensile tests with samples prepared under different conditions, the resulting estimates of the constitutive parameters (μ, g, τ_R) and P_{max} were subjected to statistical post hoc analysis. The Kruskal-Wallis test was employed to reveal deviations in the mean values. In this case, the null hypothesis states that the medians in groups A to D are equal. Subsequently, Dunn's test was used to detect differences between individual pairs of groups. A significance threshold of $\alpha = 0.05$ was applied throughout. All statistical analyses were performed using Excel (Microsoft, USA) and its add-in Real Statistics (Real Statistics Resource Pack, Release 8.9.1, https://real-statistics.com).

Horný L., Petřivý Z., Sobotka Z., Kohan M., Balint T., Chlup H., Kronek J., Mendová K., Hudák R., Schnitzer R., Danko M., Hlubeňová J. (2025) Notes on constitutive modeling of 3D-printed PLA materials. *Journal of the Mechanical Behavior of Biomedical Materials* Vol. 169, art. no. 107083. **Accepted manuscript** version distributed under CC BY-NC-ND 4.0. Link to the publisher version https://doi.org/10.1016/j.jmbbm.2025.107083.

3 Results and Discussion

A total of 23 valid tensile tests were conducted with four groups of 3D-printed PLA-PHB strips. The compositions of the samples and the number of samples in each group are presented in Table 1. Estimated material parameters and tensile strength are shown in Table 2. The results of the uniaxial tensile tests are illustrated in Fig. 3 and separately for each sample group in Fig. 4.

As can be seen from the stress-strain curves, the samples exhibited a highly non-linear, concave behaviour similar to that known for PLA-based materials (Sankaran et al., 2014b; Gonabadi et al., 2020; Lopresti et al., 2020; Custodio et al., 2021; Zarna et al., 2023; Luo et al., 2022; Foroughi et al., 2023; Mrozik and Pejkowski, 2023). While the shapes of the curves are similar for all samples, the overall stiffness varies between the sample groups. The influence of infill density is clearly evident as the 50% infill samples have significantly lower stiffness and especially the lowest strength.

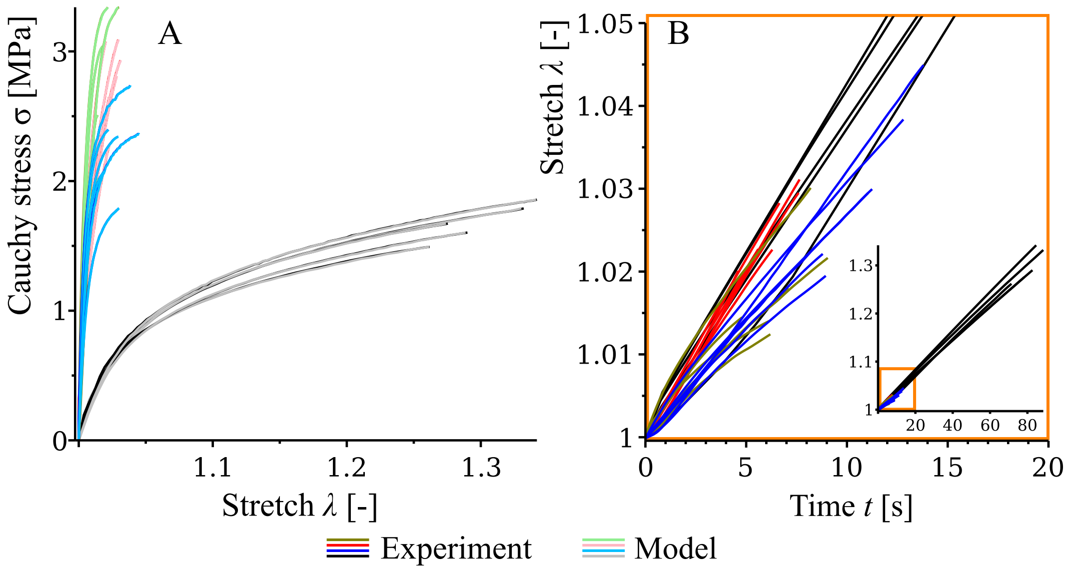

Fig. 3 – Results of all uniaxial tensile tests along with their corresponding model predictions (A). Time course of deformation of the specimens during the tensile tests (B).

The ultimate tensile strength found in the investigated groups A, B and C (100% infill) was 2.7 ± 0.54 MPa, 2.734 ± 0.30 MPa and 2.216 ± 0.303 MPa respectively, whereas in group D (50% infill) it was 1.295 ± 0.083 MPa (mean ± sample standard deviation). The comparison of groups B and C also shows that the use of a plasticiser from different manufacturers can result in different mechanical properties, even though the material composition is the same. The effect of different TAC suppliers can be attributed to the different molecular weights of TAC (402.48 g/mol for FCI vs. 360.44 g/mol for CDF).

The main aim of this study is to develop a constitutive model for the observed mechanical response. A simple QLV model was applied to fit the experimental data, and the optimized values of the constitutive parameters are presented in Table 2. The model predictions, displayed in Fig. 4, demonstrate that the model represented by equation (6) effectively reproduces the observed mechanical behavior. The coefficients of determination reported in Table 2 range from 0.977 to 0.999, with an average value of 0.992. This corresponds to a very good agreement between model and observation, and it is worth noting that this is achieved with a model that has only 3 material parameters.

Horný L., Petřivý Z., Sobotka Z., Kohan M., Balint T., Chlup H., Kronek J., Mendová K., Hudák R., Schnitzer R., Danko M., Hlubeňová J. (2025) Notes on constitutive modeling of 3D-printed PLA materials. *Journal of the Mechanical Behavior of Biomedical Materials* Vol. 169, art. no. 107083. **Accepted manuscript** version distributed under CC BY-NC-ND 4.0. Link to the publisher version https://doi.org/10.1016/j.jmbbm.2025.107083.

Table 2 – Constitutive model parameters (μ, g, τ_R) for all PLA-PHB samples, coefficient of determination R^2, and maximum nominal stress P_{max} achieved during the experiments.

		μ [MPa]	g [-]	τ_R [s]	R^2	P_{max} [MPa]
Group A	1	216.4	0.899	1.643	0.989	3.270
	2	185.7	0.893	1.750	0.998	2.985
	3	89.37	0.999	4.648	0.995	3.241
	4	101.5	0.999	6.630	0.999	2.474
	5	181.7	0.792	1.271	0.996	2.237
	6	94.22	0.793	2.251	0.999	1.992
mean ± SD		144.8 ± 56.0	0.896 ± 0.092	3.032 ± 2.137	0.996 ± 0.004	2.7 ± 0.541
Group B	1	183.2	0.954	1.075	0.996	3.015
	2	119.7	0.861	1.401	0.996	3.003
	3	113.3	0.826	1.374	0.989	2.590
	4	113.2	0.886	1.411	0.995	2.843
	5	81.56	0.867	2.276	0.999	2.731
	6	88.94	0.843	1.494	0.998	2.223
mean ± SD		116.7 ± 35.9	0.873 ± 0.045	1.505 ± 0.404	0.996 ± 0.003	2.734 ±0.30
Group C	1	140.0	0.951	1.883	0.979	2.638
	2	181.9	0.942	1.428	0.981	2.343
	3	123.1	0.941	2.067	0.993	2.275
	4	120.0	0.979	1.767	0.977	2.259
	5	166.6	0.899	1.309	0.981	2.043
	6	91.16	0.925	1.937	0.994	1.738
mean ± SD		137.1 ± 33.1	0.940 ± 0.027	1.732 ± 0.3	0.984 ± 0.007	2.216 ± 0.303
Group D	1	11.08	0.909	8.822	0.996	1.394
	2	10.18	0.901	9.953	0.997	1.343
	3	10.58	0.900	10.01	0.998	1.311
	4	10.88	0.904	8.765	0.995	1.242
	5	17.71	0.925	4.772	0.983	1.183
mean ± SD		12.09 ± 3.16	0.908 ± 0.01	8.464 ± 2.15	0.994 ± 0.006	1.295 ± 0.083

Standard hyperelastic models are able to fit the initial stiff behavior, as has been demonstrated with similar materials in the literature (Vieira et al., 2011; Shojaeiarani et al., 2019; Laycock et al., 2024). However, purely elastic models for PLA-based materials often struggle to accurately represent the response at larger strains, where the stress-strain curve flattens rapidly. They may also require an excessive number of constitutive parameters (Asfahr et al., 2023; Issabayeva and Shishkovsky, 2023; Zarna et al., 2023). This is because most strain energy density function models were developed to reproduce the large strain stiffening behavior of macromolecular chains (Holzapfel, 2000; Bergström, 2015). However, in the case of thermoplastics, dissipative phenomena play a more significant role in decreasing the slope of the tangent to the stress-strain curve at large strains compared to elastomers, where the entropic effects associated with the spatial arrangements of macromolecular chains dominate (Houwink and de Decker, 1971; Rösler et al., 2007; Brinson and Brinson, 2008).

Some works resort to the assumption of linear viscoelasticity (Lei et al., 2018; Issabayeva and Shishkovsky, 2023; Gao and Drozdov, 2024), which allows to sufficiently represent the observed behavior under uniaxial stress state. However, these models are difficult to generalize to the level of describing 3D stress and strain states. Several models have been proposed that combine both nonlinearity and viscoelasticity principles in the constitutive description (Luo et al., 2022; Adibeig et al., 2023; Foroughi et al., 2023; Mrozik and Pejkowski, 2023; Ji et al., 2024). Although these works provide results that successfully capture the experimental data, as mathematical models they are formulated within the framework of infinitesimal strain theory, which severely limits their applicability to the computational modeling of real components. Conversely, fully nonlinear models (finite strains and material) with inelastic elements, such as the Three Network Model (Bergström, 2015), require numerous material parameters. This complexity makes it difficult to design experiments and conduct subsequent regression analyses, raising concerns regarding whether a true global minimum of the objective function is reached and whether the estimated parameter values are independent of each other.

Horný L., Petřivý Z., Sobotka Z., Kohan M., Balint T., Chlup H., Kronek J., Mendová K., Hudák R., Schnitzer R., Danko M., Hlubeňová J. (2025) Notes on constitutive modeling of 3D-printed PLA materials. *Journal of the Mechanical Behavior of Biomedical Materials* Vol. 169, art. no. 107083. **Accepted manuscript** version distributed under CC BY-NC-ND 4.0. Link to the publisher version https://doi.org/10.1016/j.jmbbm.2025.107083.

An example of the application of the viscoelastoplastic Three Network Model to PLA is provided by Volgin and Shishkovsky (2021), which necessitates 12 parameters.

In contrast, this study aims to show that it is possible to model the concave behavior typical of PLA-based materials using the theory of QLV. By adopting this method, the model described in equation (6) was able to fit the data effectively. Furthermore, the model employs only three constitutive parameters, which are easily interpretable. Specifically, the model consists of an elastic spring based on the neo-Hookean hyperelastic model (parameter μ) and a relaxation component based on the Maxwell rheological element (parameters g and τ_R). This approach therefore seems appropriate in cases where a hyperelastic model gives unsatisfactory results on the one hand, but a complex nonlinear viscoelastic or viscoelastoplastic model is too robust for the problem under investigation on the other.

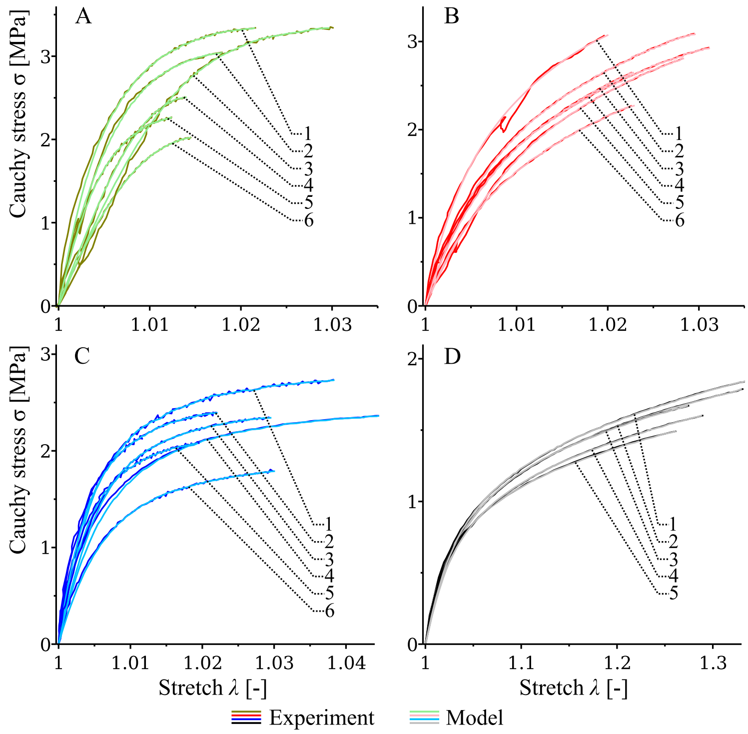

Fig. 4 – Detailed comparison of the viscoelastic models and experimental data. Specific values of the model parameters are presented in given Table 2.

The model certainly has its limitations, as its efficiency has only been demonstrated on uniaxial tensile experiments performed at a single deformation rate. Furthermore, it should be mentioned that incompressibility was assumed in order to keep the model as simple as possible, although it is not based on real observations on the tested specimens and some works show the compressible behavior of 3D printed PLA materials (Song et al., 2017). The assumption of incompressibility was only used to simplify the formulas expressing the material response. Obviously, the whole theory as given in Eqs. (1) to (5) is also ready for compressible behavior, which would lead to the need to introduce an additional parameter; see De Pascalis et al. (2014) for more details. Nevertheless, the assumption of incompressibility is commonly applied to both PLA-based and other thermoplastic materials (Rubio-López et al., 2016; Sweeney et al., 2021).

Horný L., Petřivý Z., Sobotka Z., Kohan M., Balint T., Chlup H., Kronek J., Mendová K., Hudák R., Schnitzer R., Danko M., Hlubeňová J. (2025) Notes on constitutive modeling of 3D-printed PLA materials. *Journal of the Mechanical Behavior of Biomedical Materials* Vol. 169, art. no. 107083. **Accepted manuscript** version distributed under CC BY-NC-ND 4.0. Link to the publisher version https://doi.org/10.1016/j.jmbbm.2025.107083.

3.1 Statistical Comparison of Material Parameters

To assess how printing conditions, reflected by sample groups A–D, influence the mechanical response obtained in the experiments, the Kruskal–Wallis test was performed for each constitutive model parameter (μ, g, τ_R) and ultimate tensile stress P_{max}. Table 3 summarizes the results and shows that at the significance level 0.05 differences were observed for all parameters with an exception of g. Post-hoc analysis was complemented with Dunn's test to reveal pair-wise differences which are documented in Tables 4 and 5.

Table 3. Kruskal-Wallis test of between-group results.

Parameter	p-value
μ [MPa]	**0.006**
g [-]	0.123
τ_R [s]	**0.006**
P_{max} [MPa]	**0.003**

Table 4. Dunn's pos thoc p-values for μ (above diagonal elements) and g (below diagonal elements).

	A	B	C	D
A	-	0.395	0.932	**0.002**
B	0.383	-	0.350	**0.026**
C	0.142	**0.020**	-	**0.002**
D	0.595	0.172	0.385	-

Table 5. Dunn's post hoc p-values for τ_R (above diagonal elements) and P_{max} (below diagonal elements).

	A	B	C	D
A	-	0.173	0.610	**0.032**
B	0.832	-	0.395	**0.001**
C	0.217	0.148	-	**0.009**
D	**0.002**	**0.001**	0.051	-

Statistical analysis confirms what one can derive from Fig. 3 and 4. There are differences between the groups in their mechanical responses and in terms of the constitutive model parameters. They are most significantly expressed via initial shear modulus μ and relaxation time τ_R where the Kruskall-Wallis test showed differences and the pair-wise comparison showed that all the groups differ. The differences can be explained by the different content of infill and plasticizer as follows from a comparison of Tables 3 to 5 with Table 1, which documents the preparation of materials. For the viscoelastic parameter g, although most pairwise differences were not significant, a notable exception was found between Groups B and C (p = 0.019), suggesting that even subtle changes in plasticizer composition can affect viscoelastic behavior (see the responses between Group B and C in Fig. 3A and in detail in Fig. 4B and 4C). Finally, an absence of significant differences in P_{max} between C and D group suggests that some changes in preparation conditions may compensate each other. In this case, the decrease in infill (D) is likely balanced by a decrease in molecular weight, and in the end differences in the ultimate tensile stress are statistically insignificant.

4 Conclusion

The mechanical behavior of 3D-printed samples composed of PLA, PHB, and TAC was investigated in this study. Uniaxial tensile tests were conducted on four sample groups with different material compositions. The specimens exhibited a concave behavior typical of PLA-based composites with differences in stiffness between groups, indicating a significant effect of plasticizer type and infill density.

Our study demonstrated that the theory of Quasi-Linear Viscoelasticity, which can be classified as one of the simpler approaches among fully nonlinear theories describing the inelastic behavior of solids, is capable of reproducing the experimental behavior with a relatively small number of material parameters. The model provided excellent agreement across all sample groups, highlighting its suitability for the constitutive description of PLA-based materials used in additive manufacturing.

Nevertheless, the approach has its limitations. The model was calibrated using uniaxial tensile data at a single deformation rate and under assumption of incompressibility, which may not fully represent multiaxial or rate-dependent behaviors. Future studies should explore the influence of strain rate and extend the analysis to additional deformation modes or loading conditions, such as cyclic loading, in order to assess the broader applicability of the model.

The design of the constitutive model used and its success in modeling the tensile test also suggest that the nonlinearity of the mechanical response of PLA, as demonstrated by the stress-strain curves, may not stem from the material's elastic properties, but rather from irreversible phenomena, which are represented by viscoelasticity in our model. Naturally, the model can be further refined, for instance by incorporating plastic effects; however, doing so would require introducing additional material parameters, which would counteract our original objective of demonstrating the capabilities of a three-parameter model. For this reason, we leave such extensions to future investigations.

From an application viewpoint, the simplicity and predictive accuracy of the QLV model make it a practical candidate for preliminary design and material selection processes in 3D-printed biomedical, packaging, or consumer products where PLA–PHB blends are commonly used. Furthermore, the efficient identification of viscoelastic parameters enables potential integration into the finite element simulations of printed components, especially in early-stage prototyping.

Acknowledgement

This study has been supported by the Ministry of Education, Youth and Sports of the Czech Republic in the project LUASK22174 entitled "Bioresorbable materials for additive manufacturing of vascular replacements and their biomechanical characterization ", and by the Slovak Research and Development Agency in the project SK-CZ-RD-21-0056 "Bioresorbable materials for additive manufacturing of vascular replacements and their biomechanical characterization".

References

Abdulhameed, O., Al-Ahmari, A., Ameen, W., Mian, S.H., 2009. Additive manufacturing: Challenges, trends, and applications. Advances in Mechanical Engineering 11(2). https://doi.org/10.1177/1687814018822880

Adibeig, M.R., Vakili-Tahami, F., Saeimi-Sadigh, M.-A., 2023. Numerical and experimental investigation on creep response of 3D printed Polylactic acid (PLA) samples. Part I: The effect of building direction and unidirectional raster orientation. Journal of the Mechanical Behavior of Biomedical Materials 145. https://doi.org/10.1016/j.jmbbm.2023.106025

Afshar, R., Jeanne, S., Abali, B.E., 2023. Nonlinear Material Modeling for Mechanical Characterization of 3-D Printed PLA Polymer With Different Infill Densities. Applied Composite Materials 30, 987-1001.. https://doi.org/10.1007/s10443-023-10122-y

Bergström, J., 2015. Mechanics of Solid Polymers. Elsevier, Amsterdam.. https://doi.org/10.1016/C2013-0-15493-1

Brinson, H.F., Brinson, L.C., 2008. Polymer Engineering Science and Viscoelasticity. Springer US, Boston, MA.. https://doi.org/10.1007/978-0-387-73861-1

Čajková, J., Trebuňová, M., Modrák, M., Ižaríková, G., Bačenková, D., Balint, T., Živčák, J., 2024. Influence of Oligomeric Lactic Acid and Structural Design on Biodegradation and Absorption of PLA-PHB Blends for Tissue Engineering. Polymers 16.. https://doi.org/10.3390/polym16212969

Custodio, C. L., M. Broñola, P.J., R. Cayabyab, S., U. Lagura, V., R. Celorico, J., A. Basilia, B., 2021. Powder Loading Effects on the Physicochemical and Mechanical Properties of 3D Printed Poly Lactic Acid/Hydroxyapatite Biocomposites. International Journal of Bioprinting 7.. https://doi.org/10.18063/ijb.v7i1.326

Dai, X., Li, X., Zhang, M., Xie, J., Wang, X., 2018. Zeolitic Imidazole Framework/Graphene Oxide Hybrid Functionalized Poly(lactic acid) Electrospun Membranes: A Promising Environmentally Friendly Water Treatment Material. ACS Omega 3, 6860-6866.. https://doi.org/10.1021/acsomega.8b00792

De Pascalis, R., Abrahams, I.D., Parnell, W.J., 2014. On nonlinear viscoelastic deformations: a reappraisal of Fung's quasi-linear viscoelastic model. Proceedings of the Royal Society A: Mathematical, Physical and Engineering Sciences 470.. https://doi.org/10.1098/rspa.2014.0058

De Pascalis, R., Parnell, W.J., Abrahams, I.D., Shearer, T., Daly, D.M., Grundy, D., 2018. The inflation of viscoelastic balloons and hollow viscera. Proceedings of the Royal Society A: Mathematical, Physical and Engineering Sciences 474.. https://doi.org/10.1098/rspa.2018.0102

Drapaca, C.S., Sivaloganathan, S., Tenti, G., 2007. Nonlinear Constitutive Laws in Viscoelasticity. Mathematics and Mechanics of Solids 12, 475-501.. https://doi.org/10.1177/1081286506062450

Dukle, A., Sankar, M.R., 2024. 3D-printed polylactic acid scaffolds for bone tissue engineering: Bioactivity enhancing strategies based on composite filaments and coatings. Materials Today Communications 40.. https://doi.org/10.1016/j.mtcomm.2024.109776

Farah, S., Anderson, D.G., Langer, R., 2016. Physical and mechanical properties of PLA, and their functions in widespread applications — A comprehensive review. Advanced Drug Delivery Reviews 107, 367-392.. https://doi.org/10.1016/j.addr.2016.06.012

Findrik Balogová, A., Trebuňová, M., Ižaríková, G., Kaščák, Ľ., Mitrík, L., Klímová, J., Feranc, J., Modrák, M., Hudák, R., Živčák, J., 2021. In Vitro Degradation of Specimens Produced from PLA/PHB by Additive Manufacturing in Simulated Conditions. Polymers 13.. https://doi.org/10.3390/polym1310154

Foroughi, A.H., Valeri, C., Jiang, D., Ning, F., Razavi, M., Razavi, M.J., 2023. Understanding compressive viscoelastic properties of additively manufactured PLA for bone-mimetic scaffold design. Medical Engineering & Physics 114.. https://doi.org/10.1016/j.medengphy.2023.103972

Fountas, N.A., Kitsakis, K., Aslani, K.-E., Kechagias, J.D., Vaxevanidis N.M., 2021. An experimental investigation of surface roughness in 3D-printed PLA items using design of experiments. Proceedings of the Institution of Mechanical Engineers, Part J. 236(10), 1979-1984. https://doi.org/10.1177/13506501211059306

Fountas, N.A., Kitsakis, K., Aslani, K.-E., Kechagias, J.D., Vaxevanidis, N.M., 2022. An experimental investigation of surface roughness in 3D-printed PLA items using design of experiments. Proceedings of the Institution of Mechanical Engineers, Part J: Journal of Engineering Tribology 236, 1979-1984.. https://doi.org/10.1177/13506501211059306

Fountas, N.A., Zaoutsos, S., Chaidas, D., Kechagias, J.D., Vaxevanidis, N.M., 2023. Statistical modelling and optimization of mechanical properties for PLA and PLA/Wood FDM materials. Materials Today: Proceedings 93, 824-830.. https://doi.org/10.1016/j.matpr.2023.08.276

Fung, Y.C., 1972. Stress-strain-history relations of soft tissues in simple elongation. In: Fung, Y.C., Perrone, N., Anliker, M., (Eds.), Biomechanics: Its foundations and objectives. Prentice-Hall, Inc., Englewood Cliffs, pp. 181-208.

Fung, Y.C., 1993. Biomechanics Mechanical properties of living tissues, second ed. Springer Verlag, New York

Fung, Y.C., 1994. A First Course in Continuum Mechanics: For Physical and Biological Scientists and Engineers, third ed. Prentice-Hall, Englewood Cliffs.

Gao, L., Drozdov, A.D., 2024. Exploring the performance of bio-based PLA/PHB blends: A comprehensive analysis. Polymers from Renewable Resources 15, 358-374.. https://doi.org/10.1177/20412479241266954

Garzon-Hernandez, S., Arias, A., Garcia-Gonzalez, D., 2020. A continuum constitutive model for FDM 3D printed thermoplastics. Composites Part B: Engineering 201.. https://doi.org/10.1016/j.compositesb.2020.108373

Gonabadi, H., Yadav, A., Bull, S.J., 2020. The effect of processing parameters on the mechanical characteristics of PLA produced by a 3D FFF printer. The International Journal of Advanced Manufacturing Technology 111, 695-709.. https://doi.org/10.1007/s00170-020-06138-4

Grémare, A., Guduric, V., Bareille, R., Heroguez, V., Latour, S., L'heureux, N., Fricain, J.-C., Catros, S., Le Nihouannen, D., 2018. Characterization of printed PLA scaffolds for bone tissue engineering. Journal of Biomedical Materials Research Part A 106, 887-894.. https://doi.org/10.1002/jbm.a.36289

Holzapfel, G. A., 2000. Nonlinear Solid Mechanics: A Continuum Approach for Engineering. John Wiley and Sons, Chichester.

Horakova, J., Mikes, P., Saman, A., Jencova, V., Klapstova, A., Svarcova, T., Ackermann, M., Novotny, V., Suchy, T., Lukas, D., 2018. The effect of ethylene oxide sterilization on electrospun vascular grafts made from biodegradable polyesters. Materials Science and Engineering: C 92, 132-142.. https://doi.org/10.1016/j.msec.2018.06.041

Horný, L., Vištejnová, L., Suchý, T., Kuželová Košťáková, E., Chlup, H., Kronek, J., Sobotka, Z., Petřivý, Z., Žaloudková, M., Havlíčková, K., Moláček, J., 2025. Degradation of the mechanical properties of poly-lactide-caprolactone-collagen composite for pulmonary artery banding after implantation into a rat's peritoneum. Medical Engineering & Physics 138.. https://doi.org/10.1016/j.medengphy.2025.104319

Houwink, R., de Decker, H.K., 2009. Elasticity, Plasticity and Structure of Matter, third ed. Cambridge University Press, Cambridge.

Issabayeva, Z., Shishkovsky, I., 2023. Prediction of The Mechanical Behavior of Polylactic Acid Parts with Shape Memory Effect Fabricated by FDM. Polymers 15.. https://doi.org/10.3390/polym15051162

JI, Q., Wei, J., YI, J., Zhang, L., Ma, J., Wang, Z., 2024. Study on the static and dynamic mechanical properties and constitutive models of 3D printed PLA and PLA-Cu materials. Materials Today Communications 39.. https://doi.org/10.1016/j.mtcomm.2024.108690

Kechagias, J. D., Zaoutsos, S. P., 2023. Optimising fused filament fabrication surface roughness for a dental implant. Materials and Manufacturing Processes, 38(8), 954–959. https://doi.org/10.1080/10426914.2023.2176870

Kohan, M., Lancoš, S., Schnitzer, M., Živčák, J., Hudák, R., 2022. Analysis of PLA/PHB Biopolymer Material with Admixture of Hydroxyapatite and Tricalcium Phosphate for Clinical Use. Polymers 14.. https://doi.org/10.3390/polym14245357

Lasprilla, A.J.R., Martinez, G.A.R., Lunelli, B.H., Jardini, A.L., Filho, R.M., 2012. Poly-lactic acid synthesis for application in biomedical devices — A review. Biotechnology Advances 30, 321-328.. https://doi.org/10.1016/j.biotechadv.2011.06.019

Laycock, B.G., Chan, C.M., Halley, P.J., 2024. A review of computational approaches used in the modelling, design, and manufacturing of biodegradable and biobased polymers. Progress in Polymer Science 157.. https://doi.org/10.1016/j.progpolymsci.2024.101874

Lei, D., Liang, Y., Xiao, R., 2018. A fractional model with parallel fractional Maxwell elements for amorphous thermoplastics. Physica A: Statistical Mechanics and its Applications 490, 465-475.. https://doi.org/10.1016/j.physa.2017.08.037

Lopresti, F., Campora, S., Tirri, G., Capuana, E., Carfì Pavia, F., Brucato, V., Ghersi, G., La Carrubba, V., 2021. Core-shell PLA/Kef hybrid scaffolds for skin tissue engineering applications prepared by direct kefiran coating on PLA electrospun fibers optimized via air-plasma treatment. Materials Science and Engineering: C 127.. https://doi.org/10.1016/j.msec.2021.112248

Lopresti, F., Carfì Pavia, F., Vitrano, I., Kersaudy-Kerhoas, M., Brucato, V., La Carrubba, V., 2020. Effect of hydroxyapatite concentration and size on morpho-mechanical properties of PLA-based randomly oriented and aligned electrospun nanofibrous mats. Journal of the Mechanical Behavior of Biomedical Materials 101.. https://doi.org/10.1016/j.jmbbm.2019.103449

Luo, J., Luo, Q., Zhang, G., Li, Q., Sun, G., 2022. On strain rate and temperature dependent mechanical properties and constitutive models for additively manufactured polylactic acid (PLA) materials. Thin-Walled Structures 179.. https://doi.org/10.1016/j.tws.2022.109624

Madhavan Nampoothiri, K., Nair, N.R., John, R.P., 2010. An overview of the recent developments in polylactide (PLA) research. Bioresource Technology 101, 8493-8501.. https://doi.org/10.1016/j.biortech.2010.05.092

Merodio, J., Ogden, R. (Eds.), 2020. Constitutive Modelling of Solid Continua, Solid Mechanics and Its Applications. Springer International Publishing, Cham.. https://doi.org/10.1007/978-3-030-31547-4

Mikes, P., Horakova, J., Saman, A., Vejsadova, L., Topham, P., Punyodom, W., Dumklang, M., Jencova, V., 2021. Comparison and characterization of different polyester nano/micro fibres for use in tissue engineering applications. Journal of Industrial Textiles 50, 870-890.. https://doi.org/10.1177/1528083719848155

Monaldo, E., Ricci, M., Marfia, S., 2023. Mechanical properties of 3D printed polylactic acid elements: Experimental and numerical insights. Mechanics of Materials 177.. https://doi.org/10.1016/j.mechmat.2022.104551

Mrozik, D., Pejkowski, Ł., 2023. Tensile constitutive behavior modeling of 3D printed polylactide (PLA) using visco-elastic-visco-plastic model, in: . p. 020018-.. https://doi.org/10.1063/5.0165536

Onuki, Y., Bhardwaj, U., Papadimitrakopoulos, F., Burgess, D.J., 2008. A Review of the Biocompatibility of Implantable Devices: Current Challenges to Overcome Foreign Body Response. Journal of Diabetes Science and Technology 2, 1003-1015.. https://doi.org/10.1177/193229680800200610

Ozdemir, S., Oztemur, J., Sezgin, H., Yalcin-Enis, I., 2024. Structural design and mechanical analysis of small-caliber bilayer vascular prostheses. International Journal of Polymeric Materials and Polymeric Biomaterials 1-11.. https://doi.org/10.1080/00914037.2024.2325968

Pelegrini, K., Donazzolo, I., Brambilla, V., Coulon Grisa, A.M., Piazza, D., Zattera, A.J., Brandalise, R.N., 2016. Degradation of PLA and PLA in composites with triacetin and buriti fiber after 600 days in a simulated marine environment. Journal of Applied Polymer Science 133.. https://doi.org/10.1002/app.43290

Petřivý, Z., Horný, L., 2022. Effect of viscoelasticity on inversion in axial deformation and on the volume of pressurized thin-walled tubes. European Journal of Mechanics - A/Solids 96.. https://doi.org/10.1016/j.euromechsol.2022.104763

Polanco-Loria, M., Clausen, A.H., Berstad, T., Hopperstad, O.S., 2010. Constitutive model for thermoplastics with structural applications. International Journal of Impact Engineering 37, 1207-1219.. https://doi.org/10.1016/j.ijimpeng.2010.06.006

Rajpurohit, S.R., Dave, H.K., Rajurkar, K.P., 2022. Prediction of tensile strength of fused deposition modeling (FDM) printed PLA using classic laminate theory. Engineering Solid Mechanics 10, 13-24.. https://doi.org/10.5267/j.esm.2021.12.002

Ramot, Y., Haim-Zada, M., Domb, A.J., Nyska, A., 2016. Biocompatibility and safety of PLA and its copolymers. Advanced Drug Delivery Reviews 107, 153-162. https://doi.org/10.1016/j.addr.2016.03.012

Rösler, J., Bäker, M., Harders, H., 2007. Mechanical Behaviour of Engineering Materials. Springer Berlin Heidelberg, Berlin, Heidelberg.. https://doi.org/10.1007/978-3-540-73448-2

Rubio-López, A., Hoang, T., Santiuste, C., 2016. Constitutive model to predict the viscoplastic behaviour of natural fibres based composites. Composite Structures 155, 8-18.. https://doi.org/10.1016/j.compstruct.2016.08.001

Sankaran, K.K., Krishnan, U.M., Sethuraman, S., 2014a. Axially aligned 3D nanofibrous grafts of PLA–PCL for small diameter cardiovascular applications. Journal of Biomaterials Science, Polymer Edition 25, 1791-1812.. https://doi.org/10.1080/09205063.2014.950505

Sankaran, K.K., Vasanthan, K.S., Krishnan, U.M., Sethuraman, S., 2014b. Development and evaluation of axially aligned nanofibres for blood vessel tissue engineering. Journal of Tissue Engineering and Regenerative Medicine 8, 640-651.. https://doi.org/10.1002/term.1566

Saini, P., Arora, M., Kumar, M.N.V.R., 2016. Poly(lactic acid) blends in biomedical applications. Advanced Drug Delivery Reviews 107, 47-59. https://doi.org/10.1016/j.addr.2016.06.014

Seyedsalehi, S.M., Alrashdan, A., Johnston, S., Arjunan, A., 2021. Influence of FDM process parameters on mechanical properties of PLA parts: A review. Proceedings of the Institution of Mechanical Engineers, Part C: Journal of Mechanical Engineering Science, 235(24), 7390–7405. https://doi.org/10.1177/09544062211059306

Shilov, S.Y., Rozhkova, Y.A., Markova, L.N., Tashkinov, M.A., Vindokurov, I.V., Silberschmidt, V.V., 2022. Biocompatibility of 3D-Printed PLA, PEEK and PETG: Adhesion of Bone Marrow and Peritoneal Lavage Cells. Polymers 14.. https://doi.org/10.3390/polym14193958

Shojaeiarani, J., Hosseini-Farid, M., Bajwa, D., 2019. Modeling and experimental verification of nonlinear behavior of cellulose nanocrystals reinforced poly(lactic acid) composites. Mechanics of Materials 135, 77-87.. https://doi.org/10.1016/j.mechmat.2019.05.003

Siyajeu, Y., Jiang, S., Wen, B., Li, H., 2023. Investigation on the improvement of mechanical properties and surface quality of the polylactic acid (PLA) fused filament fabrication parts manufactured without and with vibrations dependent utilization. Journal of the Mechanical Behavior of Biomedical Materials 143.. https://doi.org/10.1016/j.jmbbm.2023.105949

Song, Y., Li, Y., Song, W., Yee, K., Lee, K.-Y., Tagarielli, V.L., 2017. Measurements of the mechanical response of unidirectional 3D-printed PLA. Materials & Design 123, 154-164.. https://doi.org/10.1016/j.matdes.2017.03.051

Sweeney, J., Spencer, P., Thompson, G., Barker, D., Coates, P., 2021. Constitutive Modelling of Polylactic Acid at Large Deformation Using Multiaxial Strains. Polymers 13.. https://doi.org/10.3390/polym13172967

Trebuňová, M., Petroušková, P., Balogová, A.F., Ižaríková, G., Horňak, P., Bačenková, D., Demeterová, J., Živčák, J., 2023. Evaluation of Biocompatibility of PLA/PHB/TPS Polymer Scaffolds with Different Additives of ATBC and OLA Plasticizers. Journal of Functional Biomaterials 14.. https://doi.org/10.3390/jfb14080412

Vieira, A.C., Marques, A.T., Guedes, R.M., Tita, V., 2011. Material model proposal for biodegradable materials. Procedia Engineering 10, 1597-1602.. https://doi.org/10.1016/j.proeng.2011.04.267

Vieira, T., Afonso, A.F., Correia, C., Henriques, C., Borges, J.P., Silva, J.C., 2024. Electrospun poly(lactic acid) membranes with defined pore size to enhance cell infiltration. Heliyon 10.. https://doi.org/10.1016/j.heliyon.2024.e36091

Volgin, O., Shishkovsky, I., 2021. Material modelling of FDM printed PLA part. Engineering Solid Mechanics 153-160.. https://doi.org/10.5267/j.esm.2020.12.004

Vukasovic, T., Vivanco, J.F., Celentano, D., García-Herrera, C., 2019. Characterization of the mechanical response of thermoplastic parts fabricated with 3D printing. The International Journal of Advanced Manufacturing Technology 104, 4207-4218.. https://doi.org/10.1007/s00170-019-04194-z

Wang, Y., Luo, W., Huang, J., Peng, C., Wang, H., Yuan, C., Chen, G., Zeng, B., Dai, L., 2020. Simplification of Hyperelastic Constitutive Model and Finite Element Analysis of Thermoplastic Polyurethane Elastomers. Macromolecular Theory and Simulations 29.. https://doi.org/10.1002/mats.202000009

Weir, N.A., Buchanan, F.J., Orr, J.F., Dickson, G.R., 2004. Degradation of poly-L-lactide. Part 1: in vitro and in vivo physiological temperature degradation. Proceedings of the Institution of Mechanical Engineers, Part H: Journal of Engineering in Medicine 218, 307-319.. https://doi.org/10.1243/0954411041932782

Wineman, A., 2009. Nonlinear Viscoelastic Solids—A Review. Mathematics and Mechanics of Solids 14, 300-366.. https://doi.org/10.1177/1081286509103660

Zarna, C., Chinga-Carrasco, G., Echtermeyer, A.T., 2023. Bending properties and numerical modelling of cellular panels manufactured from wood fibre/PLA biocomposite by 3D printing. Composites Part A: Applied Science and Manufacturing 165.. https://doi.org/10.1016/j.compositesa.2022.107368

Zaoutsos, S.P., Kechagias, J.D., 2025. Optimizing bonding conditions between multilayer FFF material extrusion. Materials and Manufacturing Processes 40, 499-506.. https://doi.org/10.1080/10426914.2024.2437753